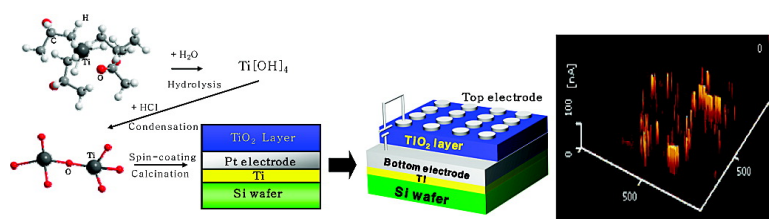


Resistive Switching Memory Devices Composed of Binary Transition Metal Oxides Using Sol-Gel Chemistry

Chanwoo Lee, Inpyo Kim, Wonsup Choi, Hyunjung Shin, and Jinhan Cho

Langmuir, 2009, 25 (8), 4274-4278 • DOI: 10.1021/la804267n • Publication Date (Web): 24 March 2009

Downloaded from <http://pubs.acs.org> on April 15, 2009



More About This Article

Additional resources and features associated with this article are available within the HTML version:

- Supporting Information
- Access to high resolution figures
- Links to articles and content related to this article
- Copyright permission to reproduce figures and/or text from this article

[View the Full Text HTML](#)

Resistive Switching Memory Devices Composed of Binary Transition Metal Oxides Using Sol–Gel Chemistry

Chanwoo Lee, Inpyo Kim, Wonsup Choi, Hyunjung Shin, and Jinhan Cho*

School of Advanced Materials Engineering, Kookmin University, and Jeongneung-dong, Seongbuk-gu, Seoul 136-702, Korea

Received December 26, 2008. Revised Manuscript Received March 9, 2009

We describe a novel and versatile approach for preparing resistive switching memory devices based on binary transition metal oxides (TMOs). Titanium isopropoxide (TIPP) was spin-coated onto platinum (Pt)-coated silicon substrates using a sol–gel process. The sol–gel-derived layer was converted into a TiO₂ film by thermal annealing. A top electrode (Ag electrode) was then coated onto the TiO₂ films to complete device fabrication. When an external bias was applied to the devices, a switching phenomenon independent of the voltage polarity (i.e., unipolar switching) was observed at low operating voltages (about 0.6 V_{RESET} and 1.4 V_{SET}). In addition, it was confirmed that the electrical properties (i.e., retention time, cycling test and switching speed) of the sol–gel-derived devices were comparable to those of vacuum deposited devices. This approach can be extended to a variety of binary TMOs such as niobium oxides. The reported approach offers new opportunities for preparing the binary TMO-based resistive switching memory devices allowing a facile solution processing.

Introduction

Nonvolatile memory devices such as charge-trap flash, phase change, ferroelectric, and resistive switching memory (RSM) have recently attracted considerable attention as the result of the widespread use of mobile electronics.^{1–12} In particular, RSM devices based on binary transition metal oxides (TMOs), which show the excellent device performance (i.e., rapid switching speed and high ON/OFF ratio, $\geq 10^3$) with a simple device structure,^{5–9} have been recognized as notable candidates for the next generation of nonvolatile memory devices since the resistance switching of oxide insulators was first introduced in 1960.¹⁰ However, these binary TMO-based devices prepared by conventional vacuum deposition have much difficulty in fabricating large-area devices, lowering production cost, and improving the process time efficiency. Recently, it was reported that perovskite magnetites, such as La_{1-x}Ca_xMnO₃, and doped perovskite oxides such as Mo-doped SrZrO₃, which were prepared by a sol–gel solution process instead of vacuum deposition, could exhibit resistive switching characteristics.^{11,12} This perovskite structure can effectively induce the lattice defects such as oxygen vacancies and interstitial

atoms, which affect the electrical properties.¹³ However, perovskite materials with multications contain the complex chemical compositions compared to the binary TMO, such as TiO₂, and the ratio of chemical compositions has a significant effect on the performance of the resistive switching properties. Hence, resistive switching materials that allow facile control of the chemical compositions as well as a solution process are needed to form the active layer of RSM devices. As an alternative, a variety of polymer-based materials such as semiconducting,¹⁴ conducting polymers,¹⁵ or nanocomposites composed of conducting components (i.e., metal nanoparticles, quantum dots, or carbon nanotubes)^{16–19} and insulating polymers²⁰ can be used as an active layer in RSM devices. Although these materials have inferior device performance and electrical stability, they have an advantage in that the active layer in RSM devices can be deposited by spin-coating with low-cost, simplified manufacturing and large area.^{21–24} Therefore, if the RSM devices composed of binary TMO materials can be easily prepared through solution processes, such as spin-coating, it is believed that such an approach can provide a critical basis for the fabrication of RSM devices with high performance and a facile manufacturing process.

*Corresponding author. E-mail: jinhan@kookmin.ac.kr.

- (1) Lee, J.-S.; Cho, J.; Lee, C.; Kim, I.; Park, J.; Kim, Y.-M.; Shin, H.; Lee, J.; Caruso, F. *Nat. Nanotechnol.* **2007**, *2*, 790–795.
- (2) Waser, R.; Aono, M. *Nat. Mater.* **2007**, *6*, 833–840.
- (3) Wuttig, M.; Yamada, N. *Nat. Mater.* **2007**, *6*, 824–832.
- (4) Rodríguez Contreras, J.; Kohlstedt, H.; Poppe, U.; Waser, R.; Buchal, C.; Pertsev, N. A. *Appl. Phys. Lett.* **2003**, *32*, 4595–4597.
- (5) Kinoshita, K.; Tamura, T.; Aoki, M.; Sugiyama, Y.; Tanaka, H. *Appl. Phys. Lett.* **2006**, *89*, 103509.
- (6) Rohde, C.; Choi, B. J.; Jeong, D. S.; Choi, S.; Zhao, J. S.; Hwang, C. S. *Appl. Phys. Lett.* **2005**, *86*, 262907.
- (7) Chae, S. C.; Lee, J. S.; Kim, S.; Lee, S. B.; Chang, S. H.; Liu, C.; Kahng, B.; Shin, H.; Kim, D.-W.; Jung, C. U.; Seo, S.; Lee, M.-J.; Noh, T. W. *Adv. Mater.* **2008**, *20*, 1154–1159.
- (8) Yun, J.-B.; Kim, S.; Seo, S.; Lee, M.-J.; Kim, D.-C.; Ahn, S.-E.; Park, Y.; Kim, J.; Shin, H. *Phys. Status Solidi (RRL)* **2007**, *1*, 280–282.
- (9) Choi, D.; Lee, D.; Sim, H.; Chang, M.; Hwang, H. *Appl. Phys. Lett.* **2006**, *88*, 082904.
- (10) Hickmott, T. W. *J. Appl. Phys.* **1962**, *33*, 2669–2682.
- (11) Zhang, T.; Su, Z.; Chen, H.; Ding, L.; Zhang, W. *Appl. Phys. Lett.* **2008**, *93*, 172104.
- (12) Lin, C.-Y.; Lin, C.-C.; Huang, C.-H.; Lin, C.-H.; Tseng, T.-Y. *Surf. Coat. Technol.* **2007**, *202*, 1319–1322.

- (13) Szot, K.; Speier, W.; Bihlmayer, G.; Waser, R. *Nat. Mater.* **2006**, *5*, 312–320.
- (14) Baek, S.; Lee, D.; Kim, J.; Hong, S.-H.; Kim, O.; Ree, M. *Adv. Funct. Mater.* **2008**, *17*, 2637–2644.
- (15) Barman, S.; Deng, F.; McCreery, R. C. *J. Am. Chem. Soc.* **2008**, *130*, 11073–11081.
- (16) Guan, W.; Long, S.; Jia, R.; Liu, M. *Appl. Phys. Lett.* **2007**, *91*, 062111.
- (17) Das, B. C.; Batabyal, S. K.; Pal, A. J. *Adv. Mater.* **2007**, *19*, 4172–4176.
- (18) Rueckes, T.; Kim, K.; Joselevich, E.; Tseng, G. Y.; Cheung, C.-L.; Lieber, C. M. *Science* **2000**, *289*, 94–97.
- (19) Verbakel, F.; Meskers, S. C. J.; de Leeuw, D. M.; Janssen, R. A. J. *J. Phys. Chem. C* **2008**, *112*, 5254–5357.
- (20) Scott, J. C.; Bozano, L. D. *Adv. Mater.* **1997**, *19*, 1452–1463.
- (21) Ouyang, J.; Chu, C.-W.; Szmanda, C. R.; Ma, L.; Yang, Y. *Nat. Mater.* **2004**, *3*, 918–922.
- (22) Tseng, R. J.; Huang, J.; Ouyang, J.; Kaner, R. B.; Yang, Y. *Nano Lett.* **2005**, *5*, 1077–1080.
- (23) Choi, S.; Hong, S.-H.; Cho, S. H.; Park, S.; Park, S.-M.; Kim, O.; Ree, M. *Adv. Mater.* **2008**, *20*, 1766–1771.
- (24) Choi, T.-L.; Lee, K.-H.; Joo, W.-J.; Lee, S.; Lee, T.-W.; Chae, M. Y. *J. Am. Chem. Soc.* **2007**, *129*, 9842–9843.

Herein we introduce a novel and versatile approach for preparing binary TMO-based RSM devices with low operating voltages, large ON/OFF ratios, long retention times, and excellent environmental stability using a sol-gel process. Titanium isopropoxide (TIPP) was used as the TiO_2 precursor for the resistive switching material, which was converted into TiO_2 after thermal annealing. The sol-gel-derived binary TMOs do not contain any additional components, such as dopants or metal nanoparticles. In addition, the electrical performance of the sol-gel-derived TiO_2 devices using the solution process was comparable to that of TMO devices produced by conventional vacuum deposition.

Experimental Section

Preparation of TiO_2 Films from Titanium Precursor. One gram of TIPP (Aldrich, 97%) was dissolved in 10 g of isopropylalcohol (IPA 99.9%). The mixed solution was hydrolyzed by dropping 0.07 g of HCl according to the procedure reported elsewhere.²⁵ These solutions were spin-coated onto Pt electrode-coated SiO_2 substrates at 4000 rpm. The resulting films were thermally annealed at 450 °C for 2 h under a nitrogen atmosphere, and further annealed at the same temperature for 4.5 h in oxygen to form anatase TiO_2 .

Surface Morphology. The surface morphology and roughness of thermally annealed TiO_2 films onto Si substrates were observed by atomic force microscopy (AFM) in tapping mode (SPA400, SEIKO).

Crystal Structure and Chemical Compositions. The crystal structure of sol-gel-derived TiO_2 films was examined using X-ray diffraction (XRD) at room temperature. Data collection was performed in the 2θ range from 15 to 60 ° using Cu $K\alpha$ radiation ($\lambda = 1.54 \text{ \AA}$, Model: Bruker D8 Discover, Germany). Cross-sectional transmission electron microscopy (TEM; model: JEOL 300kV) was also used to examine the TiO_2 crystal structure and internal structure of the nanocomposites. X-ray photoelectron spectroscopy (XPS, Sigma Probe) was carried out to determine the binding state of Ti ions and the presence of residual carbons.

Fabrication of Resistive Switching Memory Devices. All samples were prepared on Si substrates with a 100 nm thick SiO_2 layer. A 20 nm thick Ti layer was then deposited on the SiO_2 layers followed by a 100 nm thick bottom electrode (Pt) by DC-magnetron sputtering. In this case, the Ti layer was used to improve the adhesion between the SiO_2 and Pt bottom electrode. Sol-gel-derived TiO_2 and Nb_2O_5 films were then deposited on the Pt-coated Si substrates. The resulting films were thermally annealed at 450 °C for 2 h under a nitrogen atmosphere, followed by further annealing at the same temperature for 4.5 h in oxygen. After thermal conversion, 100 μm diameter Ag top electrodes were deposited on the nanocomposite films. The resistive switching behavior of the sol-gel-derived TiO_2 and Nb_2O_5 devices were examined by measuring the current-voltage ($I-V$) curves using a semiconductor parametric analyzer (SPA, Agilent 4155C) in air. The pulsed voltage duration dependence of the high and low current states was investigated using a semiconductor parametric analyzer (HP 4155A) and pulse generator (Agilent 81104A). In addition, local current maps on the nanoscale were measured using current sensing atomic force microscopy (CS-AFM) (e-sweep, SEIKO) in contact mode with conducting tips.

Results and Discussion

Sol-gel processing was performed by a hydrolysis and condensation reaction of a TiO_2 precursor solution with hydrochloric acid. The TiO_2 precursors in the sol-gel reaction were thermally annealed at 450 °C to form TiO_2 films with a concomitant mass loss of 45% due to the thermal degradation of organics (see

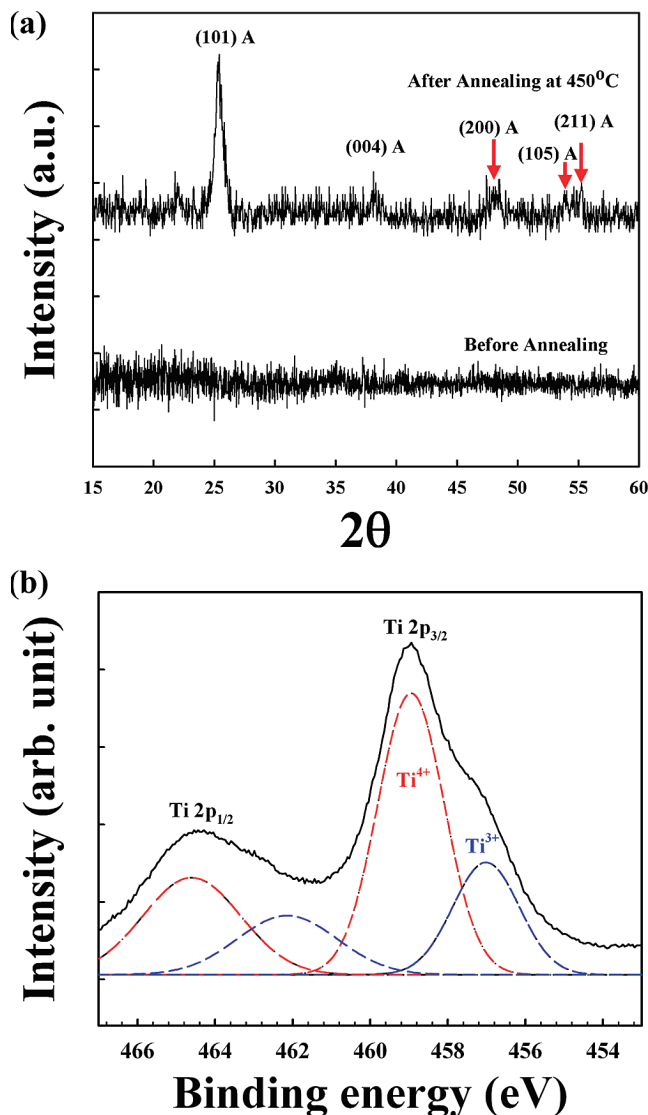


Figure 1. (a) XRD patterns and (b) the binding energy of Ti $2p_{1/2}$ and $2p_{3/2}$ were measured by XPS of TiO_2 films fabricated by sol-gel method after annealing at 450 °C.

Supporting Information Figure S1). The total film of the TiO_2 film (approximately 60.3 nm) was reduced to approximately 56.4% of the initial film thickness (approximately 107.1 nm) prior to annealing. The film thicknesses before and after thermal annealing were examined by ellipsometry and cross-section scanning electron microscopy (SEM; see Supporting Information Figure S2). The films had a low root-mean-square (rms) surface roughness of 1.15 nm in the $3 \times 3 \mu\text{m}^2$ area with the formation of anatase (see Supporting Information, Figure S3 and S4). As shown in Figure 1a, the anatase (101) XRD peak was clearly observed in the TiO_2 films grown by the sol-gel process. The XPS spectra were measured to determine the chemical composition of the films. In this case, there was almost negligible residual carbon in the sol-gel driven TiO_2 films (see Supporting Information, Figure S5). The Ti $2p_{1/2}$ and $2p_{3/2}$ XPS peaks were resolved into the two spin-orbit components, which were assigned to Ti^{4+} (458.9 eV) and Ti^{3+} (456.9 eV).²⁶ It should be noted that an oxygen-deficient state generates Ti^{3+} in TiO_2 films, and these

(26) NIST X-ray Photoelectron Spectroscopy Database, version 3.5 (Web version); Wagner, C. D., Naumkin, A. V., Kraut-Vass, A., Allison, J. W., Powell, C. J., Rumble, J. R., Eds.; National Institute of Standards and Technology: Gaithersburg, MD, 2003.

(25) Chen, X.; Mao, S. S. *Chem. Rev.* **2007**, *107*, 2891–2959.

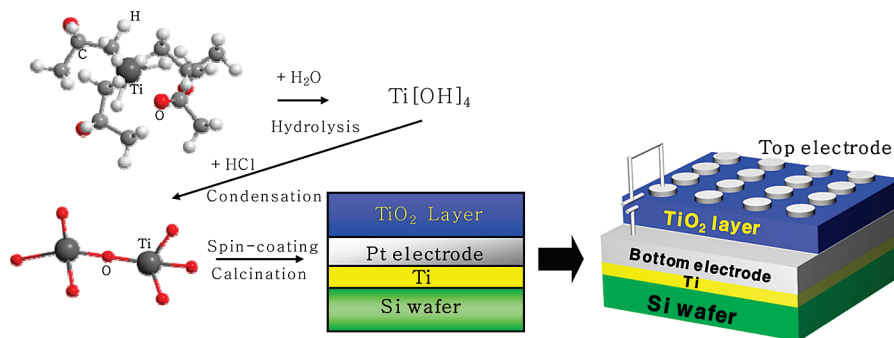


Figure 2. Schematic for RSM devices based on sol-gel-derived TiO_2 nanocomposites. A Ti layer of about 20 nm thickness was deposited for improving the adhesion between Pt electrodes and Si wafer substrates.

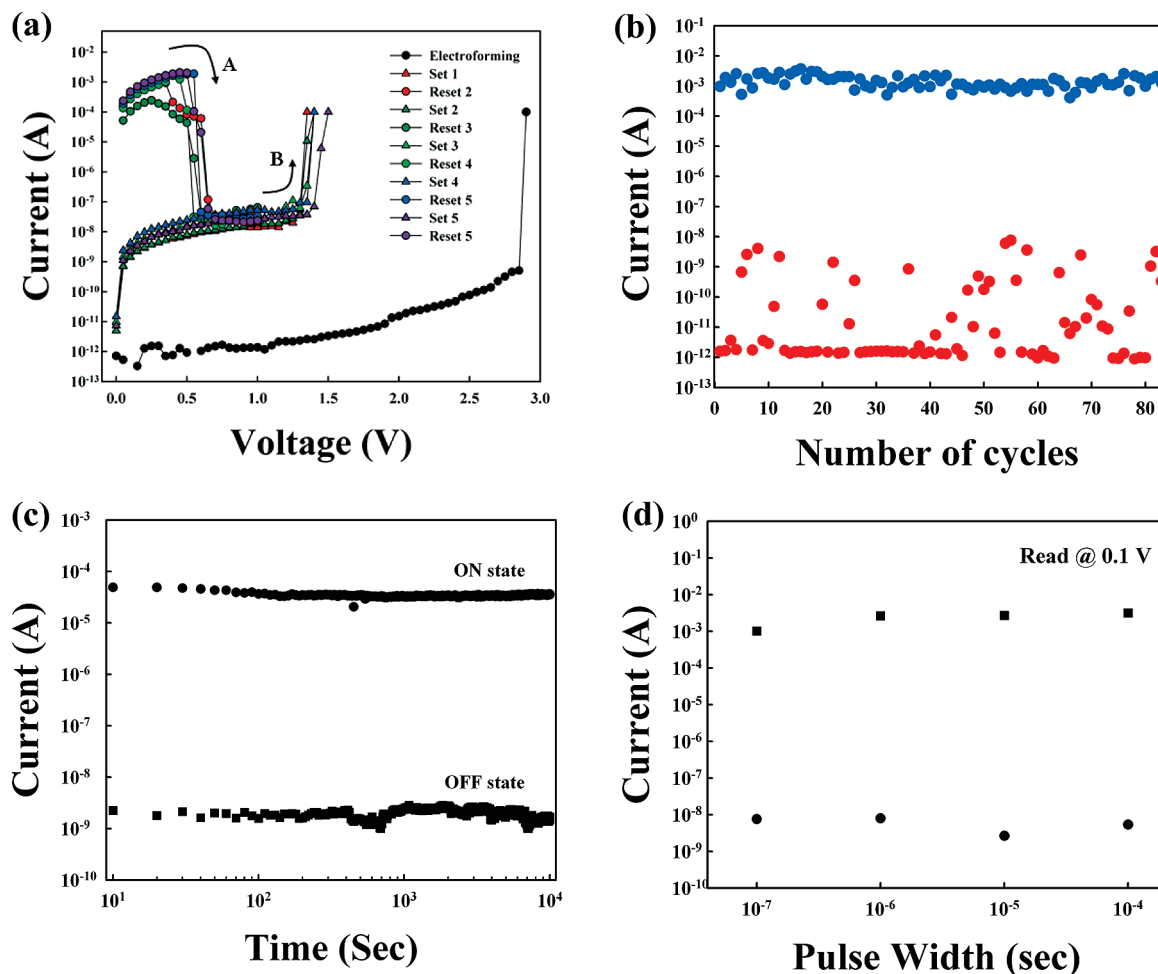


Figure 3. (a) I - V curves, (b) cycling, and (c) retention time test of sol-gel TiO_2 device showing repetitive switching cycles after initial electroforming process. (d) The current measurement with different pulse widths (100 ns, 1 μs , 10 μs , and 100 μs) for the SET process at 4 V and the RESET process at 1 V.

oxygen vacancies act as n-type dopants, transforming an insulating oxide into a semiconductor. Recently, it was reported that an applied electric field could cause the injection of electrons into the conduction band of TiO_2 , followed by reduction to metastable Ti^{3+} .^{15,27} This suggests that TiO_2 films fabricated by a sol-gel process can be used as efficient active layers in RSM devices.

On the basis of these results, an RSM device composed of the sol-gel-derived TiO_2 films was fabricated. The Ag electrodes,

approximately 100 μm in diameter, were deposited as top electrodes onto the TiO_2 films to complete device fabrication (Figure 2).

During the first sweep of the applied positive voltage, the device showed a sharp increase in current at approximately 2.9 V. The forming process of limited current compliance up to 0.1 mA, called 'electroforming', initially caused the formation of a conducting path within the TMO layers. The high current state ("ON" state) that formed after the electroforming process returned to the low current state with an abrupt decrease in current at approximately 0.6 V (i.e., V_{RESET}) during the second voltage sweep (from 0 to 1.0 V), as shown in Figure 3a (i.e., region A).

(27) Yang, J. J.; Pickett, M. D.; Li, X.; Ohlberg, D. A. A.; Stewart, D. R.; Williams, R. S. *Nat. Nanotechnol.* **2008**, *3*, 429-433.

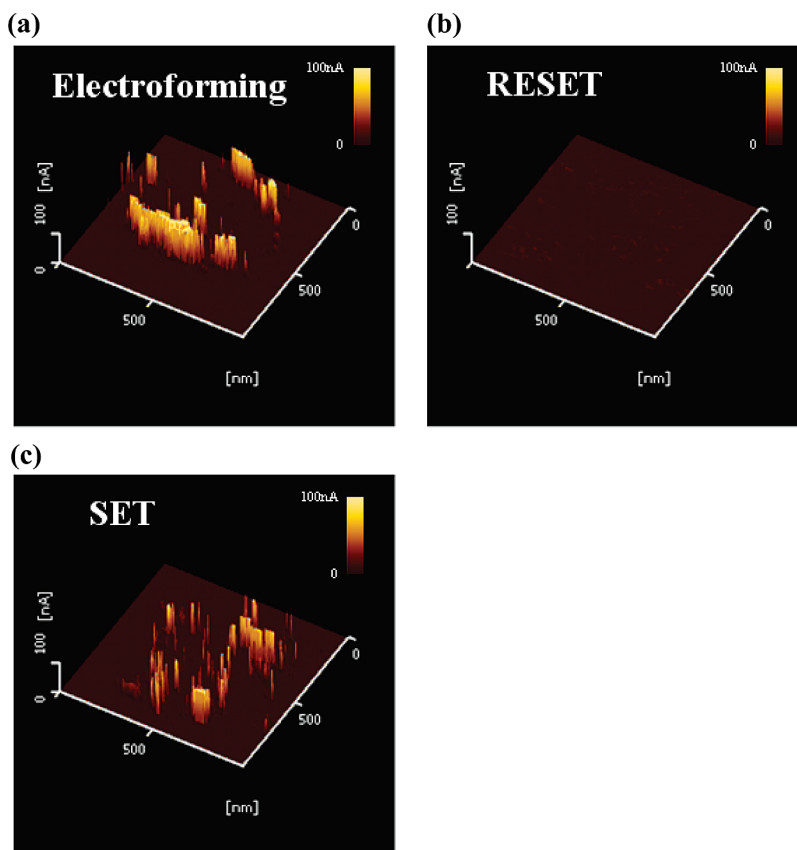


Figure 4. CS-AFM images of sol-gel-derived TiO_2 films after (a) electroforming at 10 V, (b) V_{RESET} at 2.5 V and (c) V_{SET} at 6 V.

When the applied voltage was increased again (i.e., region B), the device with the low current state (“OFF” state) showed a sharp increase in current at approximately 1.4 V (i.e., V_{SET}). This switching phenomenon, called “unipolar switching behavior”, which does not depend on the polarity and direction of the applied voltage to form the high and low current states,² can be explained by the reversible formation and disruption of the conducting filamentary path within these oxide layers, respectively. In addition, the ON/OFF ratio between the high and low current states was measured to be approximately 10^5 . It should be noted that V_{RESET} and V_{SET} of the conventional devices prepared by vacuum deposition are generally above 1 and 2 V, respectively. These results suggest that the present devices can be operated with low operating voltages and high ON/OFF ratios. A cycling test of the sol-gel TiO_2 devices was carried out in manual mode to determine their electrical stability in the ON and OFF states using a reading voltage of 0.1 V (Figure 3b). In this case, the ON and OFF states were continuously stable, maintaining high ON/OFF ratios ($> 10^4$ – 10^5) during the repeated cycling tests. To further demonstrate the stability of the resistive switching properties, data retention was gauged by examining the current level of the device in the on state over a long period of time ($> 10^4$ s) in air ambient. In this case, no appreciable change in conductivity was observed in these devices, as shown in Figure 3c. In addition, two different current states (ON and OFF states) were monitored as a function of the pulsed voltage duration (τ_p) with a pulse height of 4V and 1V, as shown in Figure 3d. The ON/OFF current ratio increased slightly with increasing τ_p from 100 ns to 100 μ s. These reversible switching properties were maintained for up to 1 year (see Supporting Information, Figure S6), demonstrating excellent electrical stability.

The local current images during the repetitive switching cycles were examined by CS-AFM to confirm the reversible formation

and disruption of the conducting filamentary paths within the sol-gel-derived TiO_2 films. For the CS-AFM measurement, CS-AFM tip (i.e., Pt tip) was used as a top electrode instead of Ag electrode. As shown in Figure 4, the formation and rupture of randomly distributed paths were observed from the electroforming, RESET and SET processes. This suggests that the current density between the top and bottom electrode is not uniform but concentrated in the localized conductive paths that are turned on and off during switching. In addition, the measured V_{RESET} of 2.5 V and V_{SET} of 6 V were higher than those from the devices shown in Figure 3a. Although not fully understood, it is believed that the surface interfacial contamination on conducting AFM surfaces may cause the additional energy barrier for the increased voltage thresholds for SET and RESET. Furthermore, the possibility that the electric field exerted from the tip is nonuniform throughout the TiO_2 layer cannot be excluded because the conducting AFM tip can be operated as an electrical point source. This nonuniform electric field can increase the applied voltages for resistive switching.

Recently, it was reported that solid electrolytes sandwiched between an Ag (or Cu) anode and an inert cathode can cause resistive switching behavior as a result of the electrochemical redox reaction based on the high mobility of Ag ions.²⁸ Although Ag electrodes were used as the top electrodes in these devices, a similar switching behavior was also observed from Pt or tungsten top electrodes (see Supporting Information, Figure S7). This indicates that the Ag electrode itself has no significant effect on the resistive switching characteristics of sol-gel-derived TiO_2 . This approach can be extended to a variety of binary TMOs as well as TiO_2 . For example, niobium ethoxide (e.g., Nb

(28) Kozicki, M. N.; Yun, M.; Hilt, L.; Singh, A. *The Electrochemical Society Proceedings Series*; Electrochemical Society: Pennington, NJ, 1999; 298–309.

(OCH₂CH₃)₅) can be also converted to Nb₂O₅ after a sol–gel reaction and subsequent thermal annealing.²⁹ When the sol–gel-derived Nb₂O₅ was used as an active layer of RSM devices, the resulting devices exhibited excellent electrical performance showing a V_{RESET} , V_{SET} and large ON/OFF ratio of approximately 0.6 V, 1.7 V, and $\sim 10^7$, respectively, as well as high electrical stability (see Supporting Information, Figure S8).

In summary, RSM devices based on binary TMO can be prepared using a facile sol–gel method. From the viewpoint of a manufacturing process and device performance, it is believed that this approach can be applied effectively to the fabrication of RSM devices with low manufacturing cost, large area deposition, and excellent electrical properties (i.e., low operating voltages, fast switching speed, and high ON/OFF ratio and electrical stability).

(29) Griesmar, P.; Papin, G.; Sanchez, C.; Livage, J. *Chem. Mater.* **1991**, *3*, 335–339.

Acknowledgment. This work was supported by a KOSEF grant funded by the Korea government (MEST) (R01-2008-000-10551-0), “SystemIC2010” project of Korea Ministry of Commerce Industry and Energy (10030559), an ERC Program of KOSEF grant funded by the Korea government (MEST) (R11-2005-048-00000-0), a Korea Research Foundation Grant funded by the Korean Government (KRF-2008-D00264), the research program 2009 of Kookmin University and NRL (R0A-2007-000-20105-0) program. We thank Prof. Hyungsang Hwang for measurements of switching speed.

Supporting Information Available: TGA, SEM, AFM, HR-TEM, XPS images of sol–gel-derived TiO₂ films; current–voltage curves of sol–gel-derived Nb₂O₅. This material is available free of charge via the Internet at <http://pubs.acs.org>.